RESEARCH PAPER

Characterization of Aluminum Matrix Composites Reinforced with Al_2O_3, SiC and Graphene Fabricated by Spark Plasma Sintering

Mohammad Jafaripour, Hassan Koohestani*, Behrooz Ghasemi

*h.koohestani@semnan.ac.ir
Faculty of Materials and Metallurgical Engineering, Semnan University

Abstract: In this study, aluminum matrix composites reinforced with Al_2O_3 and SiC nanoparticles, and graphene nanoplatelets produced by spark plasma sintering (SPS) were studied. The microstructural and mechanical properties of the composites were evaluated by changing the amounts of the reinforcing materials. The SEM images showed that the reinforcing particles were more distributed in the grain boundary regions. According to the results, the addition of alumina and SiC to the matrix caused an increase in the composite density whereas the composite density decreased by adding graphene nanoplatelets. The highest relative density of 96.3% was obtained for the composite containing 2 wt.% Al_2O_3. The presence of the reinforcing particles increased the hardness of all the samples compared to the pure aluminum (39 HV). The composite containing 1 wt.% Al_2O_3, 0.7 wt.% SiC, and 0.3 wt.% graphene showed the highest hardness of 79 HV. Moreover, the plastic deformation of the specimens decreased and the slope of the plastic region increased by adding the reinforcing particles to the matrix.

Keywords: Al composite, Spark Plasma Sintering, graphene nanoplatelets, Al_2O_3, and SiC.

1. INTRODUCTION

The ever-increasing demand for low-weight, high fuel efficiency, and high-strength materials in the automotive industry has led to the production of advanced composites. Metal matrix composites (MMCs) are extensively used in modern industries due to their mechanical behavior, tribological properties, and other desirable engineering properties [1, 2].

Among MMCs, aluminum matrix composites (AMCs) have recently attracted considerable attention in academic and industrial research. AMCs are lightweight and high-performance materials that due to enhanced strength and stiffness, improved compressive strength, increased wear resistance, increased hardness, decreased thermal conductivity, and improved dimensional stability, are a good choice for use in aerospace, defense, marine, medical, automotive, electronic packaging, and home appliances [3-5]. AMCs reinforced with particles such as silicon carbide (SiC) show improved physical and mechanical properties and can be characterized using conventional methods employed for metals [1, 2]. An increase of 1 wt.% SiC nanoparticles in Al 356 alloy while maintaining its high ductility can increase the ultimate tensile strength and yield strength by almost 100% [6].

The addition of low volume fractions of SiC particles (2-8 vol%) to an Al-12Si alloy considerably decreases in tensile strength at room temperature. As the amount of SiC content in the Al-12Si alloy increases, the weight loss due to sliding wear decreases [7]. Moreover, it was found that adding 5 vol% SiC improved the fracture strength of the aluminum matrix [8].

The first studies on the AMCs were conducted on aluminum matrix composites reinforced by SiC whiskers [9]. The applied stress can be transferred from the interface between the Al matrix and the SiC whiskers. Since the SiC whiskers act as a barrier for the movement of dislocations, the presence of whiskers improves the creep strength [10].

Another typical ceramic component for reinforcing MMCs is Al_2O_3. The effect of Al_2O_3 on the abrasion properties of the MMCs is such that the addition of Al_2O_3 reduces the wear rate of the MMCs and increasing its particle size also reduces the amount of wear [11]. As the weight percentage and particle size of Al_2O_3 increase, the density of the AMCs increases, while the porosity, tensile strength, and hardness of the AMCs increase with decreasing size and increasing the weight percentage of the Al_2O_3 particles [12].

The presence of both SiC and alumina particles exerts pressure in the grain boundary regions and thus creates intragranular tensile stress, which strengthens the grain boundaries and weakened grains. Sun et al. used a model to study the fracture mechanism of SiC-reinforced

Mohammad Jafaripour, Hassan Koohestani, Behrooz Ghasemi

composites. They found a critical SiC level at smaller quantities of which the grain boundaries were not completely reinforced, and inter-grain fracture mainly occurred along the grain boundaries. The results showed, at SiC levels larger than the critical level, the grain boundaries were relatively stronger than the grains, and hence intragranular fracture initiated from grain boundaries was dominant [13].

In addition to ceramic compounds, other compounds are also used to reinforce metal matrix composites. Among these materials, graphene with excellent thermal, electrical and mechanical properties has been proposed as an excellent reinforcement for AMCs. Several studies, with the successful production of graphene-reinforced AMCs, have shown that graphene has a positive effect on the mechanical properties of the final products and the thermal conductivity of an aluminum matrix [14-16].

Furthermore, the presence of pores and voids in composite systems negatively influences creep resistance, mechanical behaviors, and tribological properties of composites. Therefore, one must ensure that materials are completely compacted during the sintering process. Studies show that pressure-assisted fabrication techniques such as hot-pressing are usually required to compress alumina-SiC composites [17, 18].

Spark plasma sintering (SPS) can provide a low-temperature, time-saving, low-pressure, and high-quality method for the fabrication of composites [15, 19]. Therefore, for the production and research of advanced materials as well as development in the powder metallurgy industry, this method has attracted a lot of attention [17, 18, 20, 21]

In the current work, the effect of simultaneous addition of Al_2O_3, SiC and graphene reinforcements on the mechanical properties of the aluminum matrix composites produced by the SPS method is investigated. Structural and mechanical analyses were performed to study and characterize the manufactured composites.

2. EXPEROMENTS

2.1. Raw materials

Aluminum powder (ECKA, Germany), Al_2O_3 nanoparticles (NPs) (Evonik Industries, Germany), graphene NPs (US Research Nanomaterials Inc.), and SiC NPs (US Nano Inc.) were used to produce the composites. The characteristics of the utilized powders are listed in Table 1.

2.2. Composites production

2.2.1. Powder preparation

Eight composite samples containing various levels of the reinforcing particles were prepared (Table 2).

Table 1. Specifications of used powders.

Powder	Particle size	Purity	Density (g/cm³)*	Melting Point (°C)
Al	<30 micron	>99.9%	2.71	660
Al_2O_3	20 nm	99.7%	3.95	2072
SiC	40 nm	99.9%	3.21	2370
Graphene	2-18 nm	>99.5%	2.27	>4000
* Ref. [15, 22]				

Table 2. Specifications of prepared samples.

Sample	Competition (wt%)	Amount per 10 g sample (g)			
		Al	Al_2O_3	Graphene	SiC
S1	Pure Al	10	0	0	0
S2	Al-2% Al_2O_3	9.8	0.2	0	0
S3	Al- 1% Al_2O_3- 0.9% SiC- 0.1% Graphene	9.8	0.1	0.01	0.09
S4	Al- 1% Al_2O_3- 0.7% SiC- 0.3% Graphene	9.8	0.1	0.03	0.07
S5	Al- 1% Al_2O_3- 0.5% SiC- 0.5% Graphene	9.8	0.1	0.05	0.05
S6	Al- 1% Al_2O_3- 0.3% SiC- 0.7% Graphene	9.8	0.1	0.07	0.03
S7	Al- 1% Al_2O_3- 0.1% SiC- 0.9% Graphene	9.8	0.1	0.09	0.01
S8	Al- 1% Al_2O_3 -1% SiC- 2% Graphene	9.6	0.1	0.2	0.1

First, the powder mixture was dispersed in 100 mL of 99% ethanol and then ultrasonicated for 60-70 min until completely uniform. The samples were then heated in an oven at 60-70°C for 36 h to remove alcohol and obtain a dry powder mixture. Then, to better mix the powders, they were milled for a limited time in a high-energy planetary ball mill (RETSCH, Germany) at room temperature under argon. The milling parameters were: ball to powder ratio: 10:1; powder mass: 15 g; the mass of balls: 150 g; ball diameter: 15 and 10 mm; material of ball and cup: hardened stainless steel; time: 120 min and rotation: 360 rpm. Before grinding, 0.5wt.% stearic acid was added to prevent cold sintering of particles.

2.2.2. Preparation of bulk composites

Disc specimens with a diameter of 50 mm and a thickness of 2-3 mm were prepared by the SPS machine (a 10-ton model manufactured by the Iranian Company KHPF), mandrel, and graphite die. To this end, 15 g of the powder mixture was poured into a 50 mm diameter graphite die. An ISG-M303 graphite die was used with a thermocouple hole drilled into a punch. For easy separation of the sintered pellet sample and to prevent sticking (due to possible reaction between the powder and graphite die/punch from possible reactions between the powder and mandrel/die), sheets of graphite paper between the die and the powder as well as between inner wall of die and the powder were placed. The parameters used for sintering the composite samples are heating rate: 100°C/min; cooling rate: 100°C/min; the temperature of sintering: 550°C; time of sintering: 200 s and pressure: 45 MPa. A pulse direct current was applied in 360 ms and 90 ms pulse durations.

Following the sintering process, the composite discs were cleaned and the remains of the graphite sheets were removed from the surface. The surface of the discs was then sanded with #600 grit sandpaper to obtain the discs with an approximate thickness of 2 mm.

2.3. CHARACTERIZATION

2.3.1. Structural properties

X-ray diffraction (XRD, Bruker D8 diffractometer, Germany) was used for phase analysis of the composites. The fracture surface, the surface morphology of the samples, and the EDX map showing the distribution of elements

were investigated using a scanning electron microscope (SEM, Philips XL 30, the Netherlands). The density of composites was calculated using Archimedes' principle based on standard ASTM B 962-14. The theoretical density of the specimens was calculated using the following equation [22]:

$$d_{app} = \left(\frac{W_a}{W_a - W_w} \right) . \rho \qquad (1)$$

where d_{app} represents the apparent density, W_α is the sample weight in the air, W_w is the sample weight in water, and ρ shows the density of distilled water at 25°C (0.998 g/cm³). The relative density (d_r) was obtained from Eq. 2:

$$d_r = \left(\frac{d_{app}}{d_t} \right) . \rho \qquad (2)$$

where d_t denotes the theoretical density. The d_t of the composites can be determined by using the following equation:

$$d_t = \frac{1}{\sum_{i=1}^{n} \left(\frac{w_i}{\rho_i} \right)} \qquad (3)$$

Where w_i and ρ_i are the weight fraction and density of component i. The density of Al, Al_2O_3, SiC, and graphene are 2.71, 3.89, 3.22, and 2.27 g/cm³, respectively. The relative porosity was calculated from Eq. 4 employing the theoretical density and the apparent density. At the same volume, the relative porosity can be defined as the ratio of the mass of any volume of a material to that of an equal volume of water [22, 23]:

$$P_r = \left(\frac{d_t - d_{app}}{d_t} \right) . 100 \qquad (4)$$

2.3.2. Mechanical properties

To study the tensile properties of the specimens, the uniaxial tensile test on a wire-cut electric discharge machine was conducted by ASTM-E008 (on a Universal Testing Machine, Hounsfield H25KS). For each composite code, at least three specimens were used in the tensile test to ensure the repeatability of the results.

The hardness of the samples was determined and compared using a Buehler Micromet II microhardness machine employing a Vickers indenter at the load of 100 g and duration of 30 s.

This test was repeated 10 times on each sample and the average of the results was used to increase the accuracy and reliability of the results.

3. RESULTS AND DISCUSSION

Figure 1 shows the changes in temperature and puncture displacements as a function of sintering time. The densification behavior of the composites is observed during the sintering process through punch displacement. Positive values in punch displacement correspond to sample shrinkage. The maximum displacement is recorded at the highest process temperature.
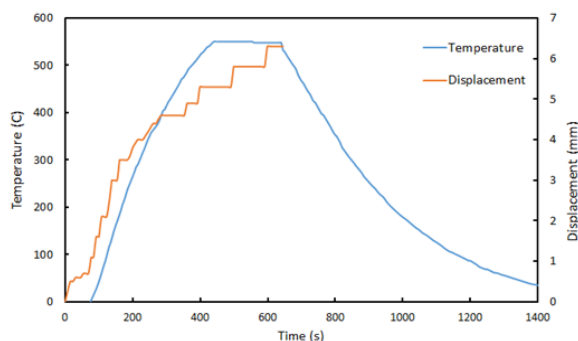
Fig. 1. The processing temperature and the punch displacement as a function of the sintering time.

Figure 2 illustrates the XRD patterns of various composite samples. In the XRD pattern of specimen S1 containing no reinforcing materials, no peaks related to the presence of impurities are observed. Therefore, it can be concluded that specimen S1 is pure aluminum (JCPDS No. 004–0787).
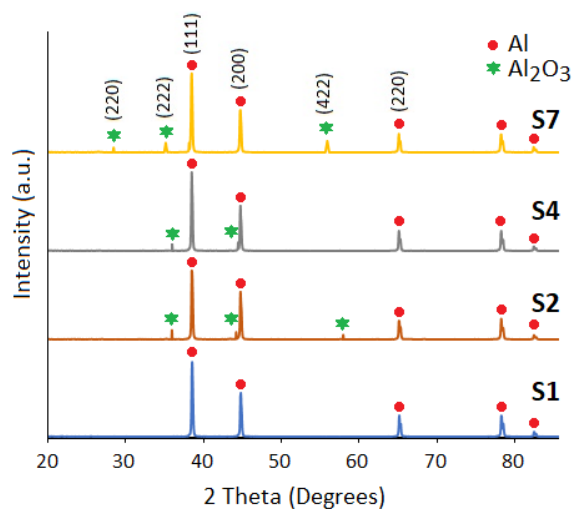

**Fig. 2.** XRD patterns of S1, S2, S4 and S7 samples.

However, in the composite specimens of S2 and S4, the peaks related to Al_2O_3 (JCPDS No. 79-1558) are observed. SiC NPs and graphene nanoplatelets, in addition to Al_2O_3, were utilized in producing the specimens S4 and S7, but the peaks related to Al_2O_3 were only found in their XRD patterns. The absence of the peak related to SiC (JCPDS No. 29-1129) and graphene in the XRD pattern could be due to their very low amount. The XRD results demonstrate the lack of reactions between the reinforcing particles and the Al matrix. Previous studies have reported the formation of gaseous reaction products (such as SiO_2, Al_2OC, and CO) in the reactions between SiC and Al_2O_3 at high temperatures [24]. Nevertheless, no reaction occurred in the detection limit of the XRD spectrometer in this study due to the absence of any additional peak in the XRD patterns. The presence of reinforcing materials such as Al_2O_3 and other additives in the structure could influence the mechanical properties of the composite specimens. This was evaluated through mechanical tests.

Figures 3 and 4 show the SEM images taken from the surface of all composite samples. The presence of the reinforcing particles in the Al matrix caused a change in the microstructure and morphology of the samples. This could influence the mechanical and tribological properties of the resulting composites. As clearly shown in Fig. 2, the pure Al sample has a smooth surface free of any reinforcing phase. Therefore, dislocation movements would take place easily in this sample. Therefore, it was expected not to exhibit desirable mechanical behavior. In the specimens reinforced with various particles, the presence of these particles changed both the grain morphology and size. According to the literature, Al_2O_3 particles attract SiC particles inside them leading to their entrapment inside alumina [9].

The composite specimens showed that the reinforcing particles were distributed mainly in the grain boundary regions. This could affect the mechanical properties of the composites. The presence of particles such as graphene and alumina in the structure of the samples locked displacement movements and hence increased their strength compared to the specimens lacking any reinforcing material. The reinforcing particles in specimen S4 accumulated in the grain

boundaries leading to an improvement in its   mechanical properties.
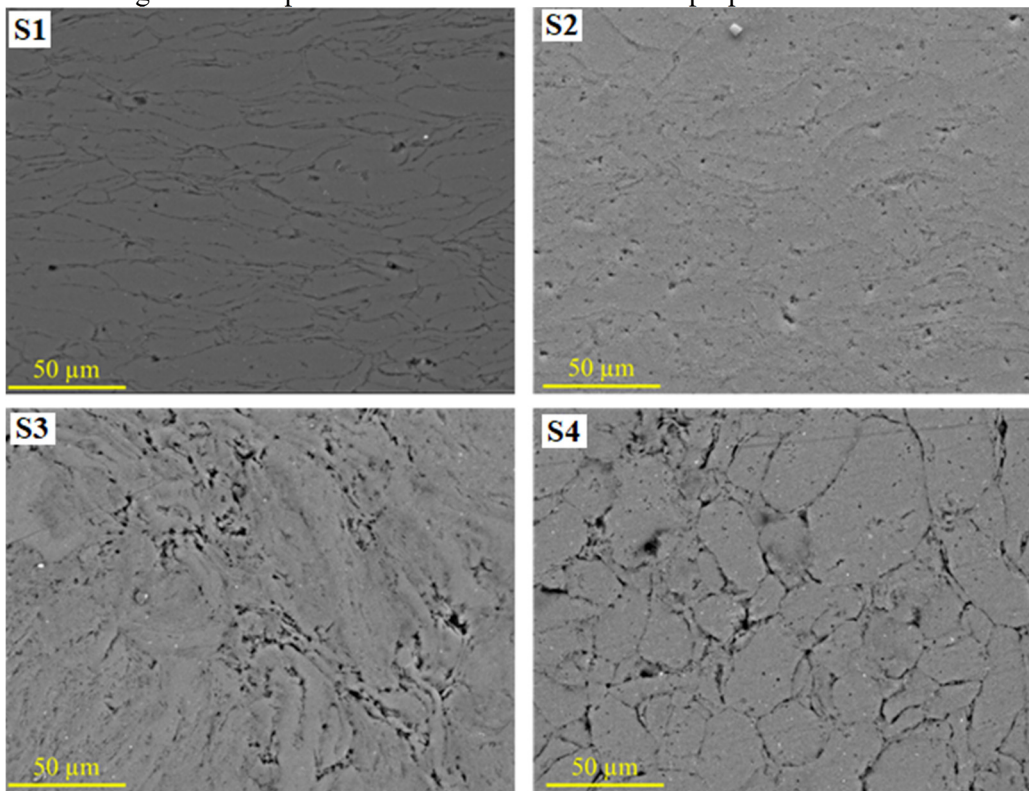
Fig. 3. SEM images of S1, S2, S3 and S4 samples.
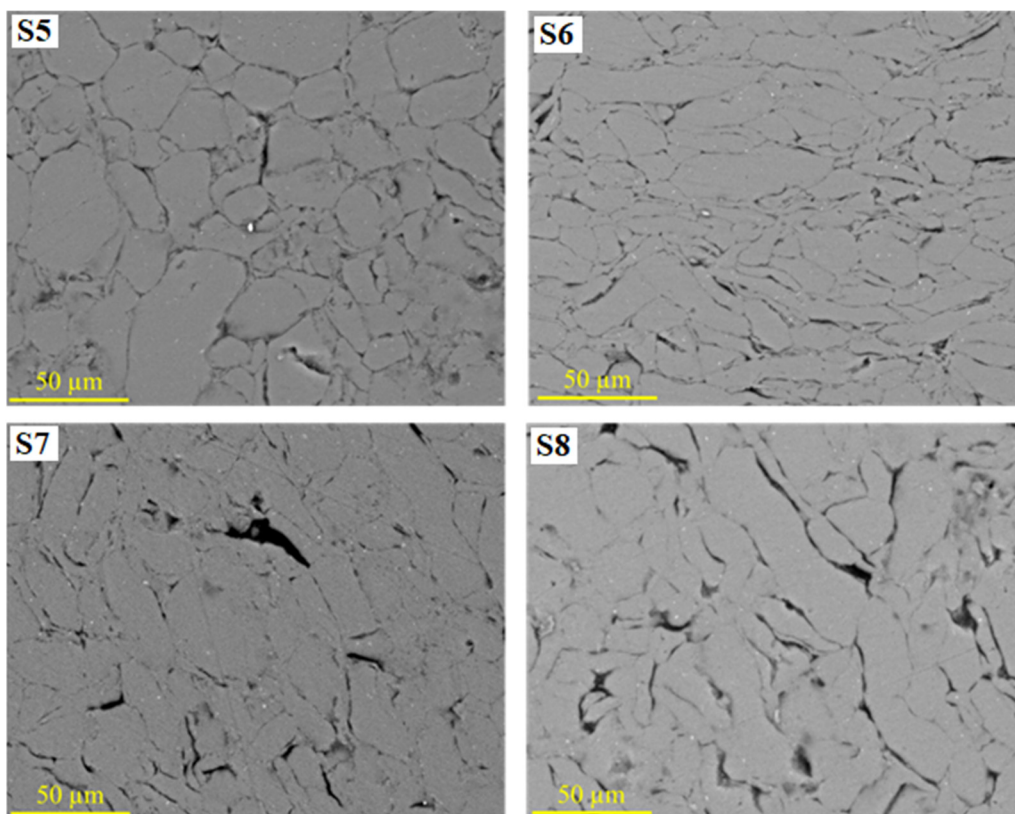
Fig. 4. SEM images of S5, S6, S7 and S8 samples.

Moreover, except for specimen S4, the other composites showed a regular structure. The presence and deposition of reinforcing particles at the grain boundaries caused substantial changes in the mechanical properties of specimen S4. The presence of these particles influenced dislocation movements via several mechanisms causing an improvement in the mechanical properties of the composite specimens. This will be discussed when the mechanical properties of the samples are studied.

According to the literature, agglomeration of reinforcing particles in composite systems is one of the most important reasons causing a decline in the engineering properties of the produced composites. Map analysis was used to study the distribution of the reinforcing particles in the structure of composites. Figure 5 shows the results of the map analysis for specimen S8. Map analysis shows the distribution of elements at the sample surface and the accumulation of reinforcing compounds at the grain boundary. The table in Figure 5 shows the weight percentage of elements in the image and at three points of the

grain boundary (points A, B, and C). As can be seen, the percentage of elements of reinforcing compounds at the grain boundary is higher than the average of the same elements in the whole image. This indicates the accumulation of reinforcing particles at the grain boundaries. This has happened to most graphene so that most of the graphene is at the grain boundary.

Figure 6 displays the fracture surface morphology of the specimens S4 and S8. It suggests a different mechanism of hardening including crack deflection, SiC and graphene whisker bridging, and protruding in this specimen. Large graphene shells in the fracture surface improve the length of crack deflection. EDX results at different points of the fracture edges show that the amount of carbon element is higher than the total percentage of carbon in the sample, considering that the amount of silicon has not changed significantly, so it can be concluded that graphene accumulation was higher in these points. Consequently, graphene can be considered a desirable reinforcing material for strengthening alumina-SiC composite [25].
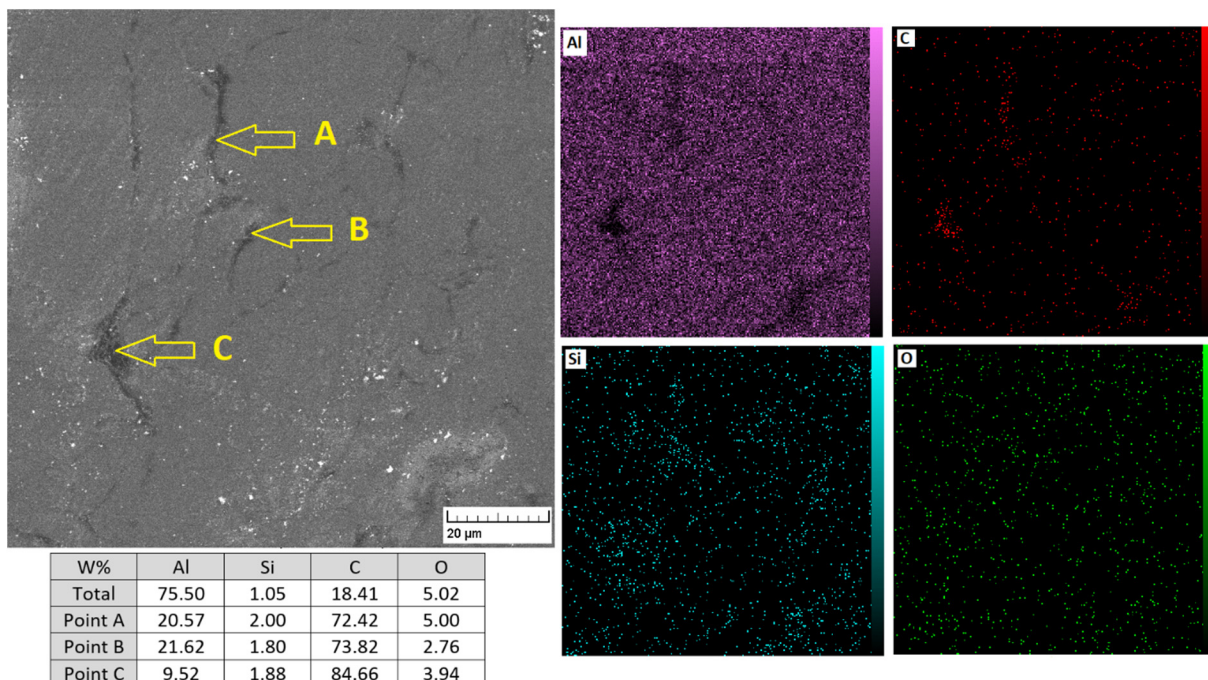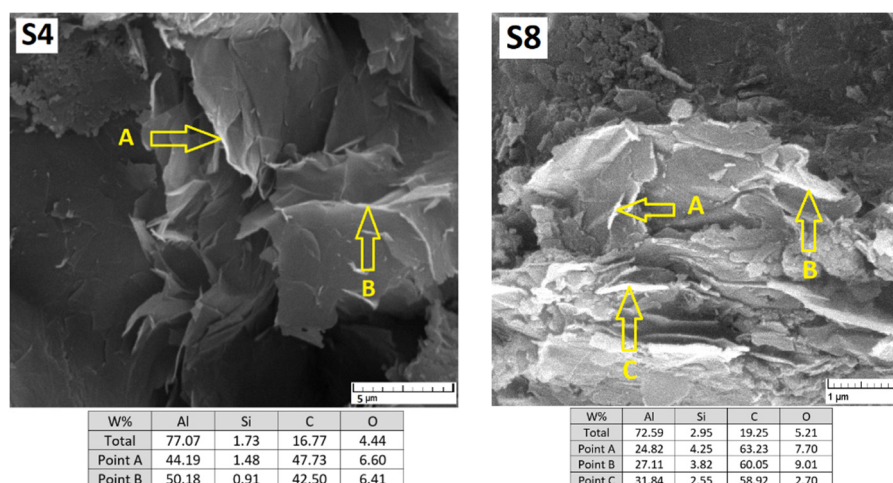

W%	Al	Si	C	O
Total	75.50	1.05	18.41	5.02
Point A	20.57	2.00	72.42	5.00
Point B	21.62	1.80	73.82	2.76
Point C	9.52	1.88	84.66	3.94

Fig. 5. SEM, map and EDX analysis of S8 sample.

Fig. 6. SEM image and EDX of fracture surface of specimen S4 and S8.

Table 3 lists the changes in the density and porosity of the various SPS samples. The results for specimens S1 and S2 show that the addition of the alumina reinforcing material to the aluminum matrix causes an increase in the relative density and a decrease in the relative porosity. However, replacing part of alumina with graphene and SiC decreased the relative density and increased the relative porosity of the composite specimens. The densities of alumina, SiC, graphene nano-platelets, and pure aluminum are 3.95, 3.21, 2.3, and 2.7 g/cm^3, respectively. Therefore, the addition of alumina and SiC to the matrix decreased the composite density, whereas the addition of graphene caused a decrease in the composite density. According to the results, the highest relative density of 93.7% and the highest relative porosity of 6.3% were obtained for specimen S8.

Porosity tends to reduce the mechanical properties of metal matrix composites. The formation of porosity, which depends on the composition and structure of the matrix, has a significant effect on the elastic modulus, yield strength, ultimate tensile strength, and ductility of composites [26]. Cramer et al. investigated the effect of pore distribution on the mechanical properties of aluminum sheets containing multiple holes by experimental study. The results showed that the overall elastic properties were almost insensitive to the actual pore-uniform distribution or the pore clusters. However, the fracture toughness of the specimens is strongly affected by the mutual position of the individual pores [27]. Porosity can significantly reduce compressive yield stress but does not change the fundamental characteristics of grain-size dependence [28].

Table 3. Density, porosity and tensile strength of all prepared samples.

Sample	d_{app} (g/cm^3)	d_r (%)	Porosity (%)	tensile strength (MPa)
S1	2.55	94.1	5.9	98
S2	2.61	96.3	3.7	134
S3	2.59	95.6	4.4	168
S4	2.59	95.6	4.4	177
S5	2.56	94.5	5.5	79
S6	2.57	94.8	5.2	78
S7	2.56	94.5	5.5	96
S8	2.54	93.7	6.3	61

Figure 7 compares the hardness of samples containing reinforcing particles. As clearly seen, the presence of the reinforcing particles increases the hardness of all the specimens compared to pure aluminum (39 HV). This means that the presence of the reinforcing particles in the composite improves the mechanical properties of the specimens. Similar results were obtained in other studies [29, 30]. Specimen S4 with a hardness of 79 HV showed the highest hardness among the specimen. This could be due to the effective presence of the reinforcing particles in suitable sites in the structure of the related specimen. The specimens with a higher relative porosity exhibited a lower hardness. Hossain et al. [31], noticed that the hardness and density of SiC and Al_2O_3 reinforced aluminum samples were interrelated. They proved that the reinforcing particles changed the relative density and increased the hardness. According to the literature, the force applied to a composite structure is distributed between the metal matrix and the reinforcing particles. In the hardness test, a vertical force is applied to the structure, and the applied stress is divided between the metal matrix and the reinforcing particles. Therefore, the stress applied to the metal matrix is reduced to apply changes in the plastic structure.
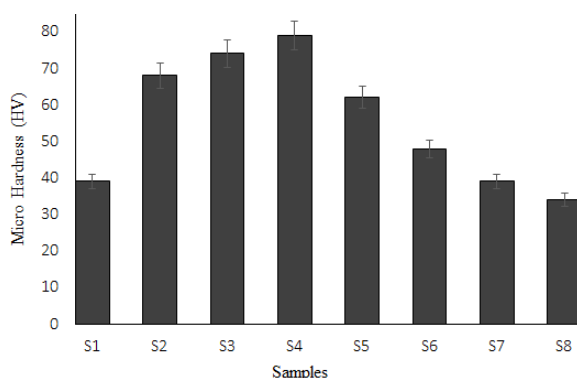

Fig. 7. Micro-hardness of all samples.

According to the results, Al_2O_3 particles play an important role in increasing the hardness so that the hardness of the specimen S2 was about twice that of pure aluminum. However, graphene decreased the hardness. In the specimen S8 contained 2% graphene, the hardness (34 HV) was lower than the other composites and even lower than pure aluminum. The addition of the optimum amount of SiC (0.7%) and graphene (0.3%) together with alumina caused specimen S8

to have the highest hardness. Dwivedi et al. found that the simultaneous addition of the optimum amounts of Al_2O_3 and SiC increased the aluminum hardness by up to 82 BHN [32]. In fact, the reinforcing particles used in this study had strong structures and lower plasticity compared to the matrix (aluminum). Therefore, the major part of the stress applied to the structure is transferred to the reinforcing particles, and hence less stress is used to deform the aluminum matrix. Therefore, the presence of reinforcing particles in the aluminum matrix increased the hardness of the samples. The appropriate amount of these particles and their deposition at the grain boundary increases the dislocation locking, the hardness of the structure increased significantly.

The increased hardness caused by the presence of the second phase can be explained by several mechanisms. The changes in the texture, in the energy of the grain boundaries in the presence of the secondary phase (the Hall-Petch relation), and dispersion strengthening (Orowan's theory) are among the reasons offered for the increase in the hardness caused by the presence of secondary particles [33-36]. Orowan strengthening depicts the effect of dimensions and inter-particulate spacing of secondary-phase dispersoids. This mechanism, caused by the resistance of closely spaced reinforcements to the passing of dislocations, is important for aluminum matrix nanocomposite but is not a significant strengthening factor for traditional metal matrix composites at room temperature [37, 38]. According to Orowan's theory, the presence of Al_2O_3, SiC and graphene cause dislocation locking and prevent their movements and, eventually, lead to increased hardness of the specimens. The increased hardness of the composite samples has also been proved in several other studies [39, 40].

Figure 8 presents the results of the tensile test for the prepared samples. It shows that the specimen S1 lacking any reinforcing particle for manufacturing the composite exhibited the highest plastic deformation. It was also observed that the presence of these particles in the specimens severely reduced plastic deformation and increased the slope of the elastic region. This indicated that the presence of the reinforcing particles increased the strength and reduced the plasticity of the specimens. The increase in the strength in the presence of the reinforcing particles can be attributed to locking and accumulation of dislocations..
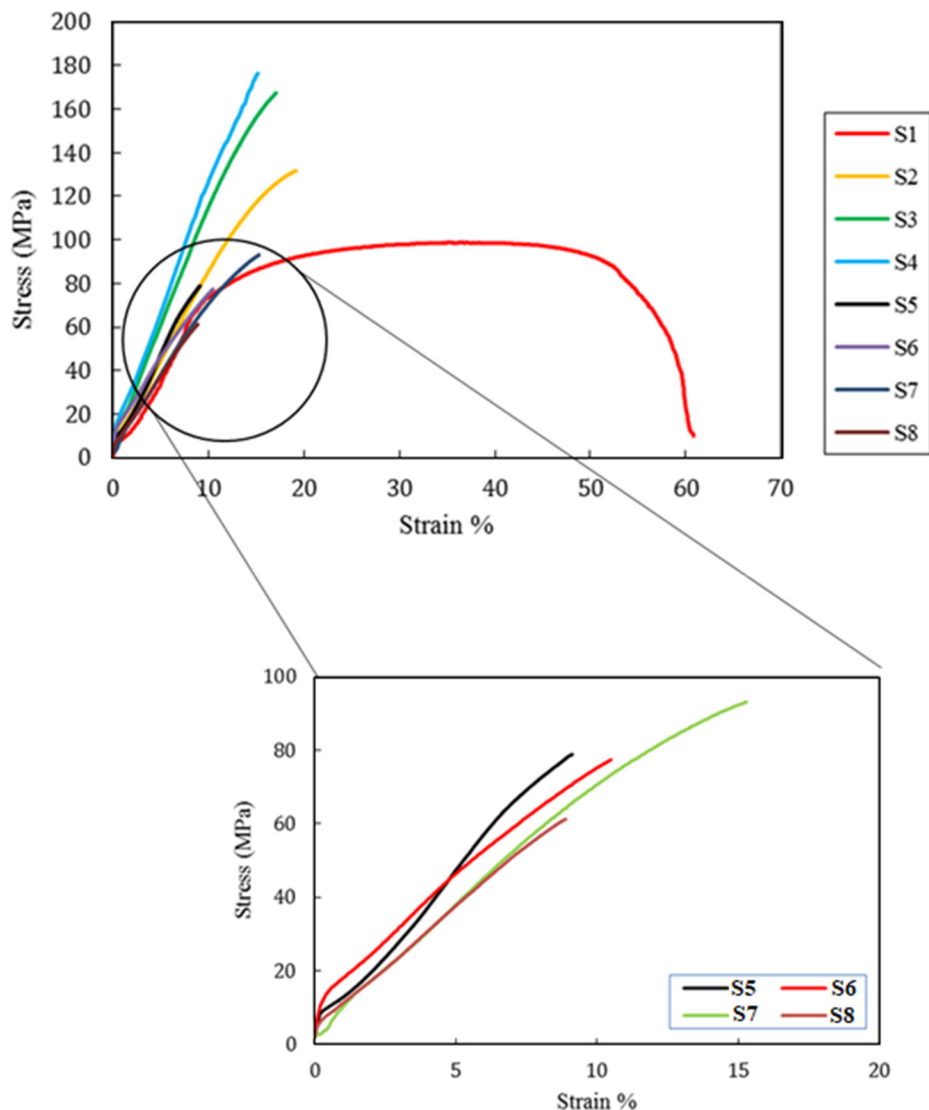
Fig. 8. The stress-strain curve obtained from the tensile test for all samples.

Table 3 lists the tensile strength values of all samples. It is clear that nanosized reinforcements have a significant effect on the tensile strength of nanocomposites. The enhanced strength of the nanocomposite is attributed to the stronger diffusional bonds and homogeneous distribution of reinforcements in the aluminum matrix during spark plasma sintering. Homogenous and uniform distribution of reinforcements in the aluminum matrix leads reinforcements to act as a barrier to the dislocations movement strengthening the matrix through the creation of high dislocations density regions during cooling at room temperature

4. CONCLUSIONS

The present study successfully produced aluminum matrix composites reinforced with Al_2O_3, SiC, and graphene using Spark Plasma Sintering (SPS). The structural and mechanical properties of composites were investigated. The results showed that the addition of reinforcing particles increases the density and reduces the porosity of the composites. It was correctly proved that the samples with less relative porosity had more hardness. The composite containing 1 wt.% Al_2O_3, 0.7 wt.% SiC, and 0.3 wt.% graphene showed higher hardness than other composites. In fact, the force applied to the composite structure is distributed between the metal matrix and the reinforcing particles. However, the presence of reinforcing particles severely reduces the plastic deformation and increases the slope of the elastic region.

REFERENCES

[1] Suresh, S. Mortensen, A., and Needleman, A., Fundamentals of metal-matrix composites. Butterworth-Heinemann, USA, 1993, 297-326.

[2] Deuis, R., Subramanian, C., and Yellup, J., "Dry sliding wear of aluminium composites-a review." Compos. Sci. technol., 1997, 57(4), 415-435.

[3] Aynalem, G.F., "Processing Methods and Mechanical Properties of Aluminium Matrix Composites." Adv. Mater. Sci. Eng., 2020, 2020, 1-19.

[4] Dash, K., Sukumaran, S., and Ray, B.C., "The behaviour of aluminium matrix composites under thermal stresses." Sci. Eng. Compos. Mater., 2016, 23(1), 1-20.

[5] Liu, J., Khan, U., Coleman, J., Fernandez, B., Rodriguez, P., Naher, S. and Brabazon, D., "Graphene oxide and graphene nanosheet reinforced aluminium matrix composites: Powder synthesis and prepared composite characteristics." Mater. Des., 2016, 94, 87-94.

[6] Pramanik, A. and Basak, A., "Fracture and fatigue life of Al-based MMCs machined at different conditions." Eng. Fract. Mech., 2018, 191, 33-45.

[7] Tjong, S., Wu, S., and Liao, H., "Wear behaviour of an Al-12% Si alloy reinforced with a low volume fraction of SiC particles." Compos. Sci. Technol., 1998, 57(12), 1551-1558.

[8] Niihara, K., Nakahiral, A., Uchiyama, T., and Hirai, T., Fracture Mechanics of Ceramics. 1986, Springer, 103-116.

[9] Álvarez, I., Torrecillas, R., Solis, W., Peretyagin, P., and Fernández, R., "Microstructural design of Al2O3-SiC nanocomposites by spark plasma sintering." Ceram. Int., 2016, 42(15), 17248-17253.

[10] Xia, K. and Langdon, T.G., "Fracture behaviour at elevated temperatures of alumina matrix composites reinforced with silicon carbide whiskers." J. Mater. Sci., 1996, 31(20), 5487-5492.

[11] Yılmaz, O. and Buytoz, S., "Abrasive wear of Al2O3-reinforced aluminium-based MMCs." Compos. Sci. Technol., 2001, 61(16), 2381-2392.

[12] Kok, M., "Production and mechanical properties of Al2O3 particle-reinforced 2024 aluminium alloy composites." J. Mater. Process. Technol., 2005, 161(3), 381-387.

[13] Sun, X., Li, J.G., Guo, H., Xiu, Z., Duan, K., and Hu, X.Z., "Intragranular particle residual stress strengthening of Al2O3-SiC nanocomposites." J. Am. Ceram. Soc., 2005, 88(6), 1536-1543.

[14] Wang, J., Li, Z., Fan, G., Pan, H., Chen, Z., and Zhang, D., "Reinforcement with graphene nanosheets in aluminum matrix composites." Scr. Mater., 2012, 66(8), 594-597.

[15] Tian, W.-m., Li, S., Wang, B., Chen, X., Liu, J., and Yu, M., "Graphene-reinforced aluminum matrix composites prepared by spark plasma sintering." Int. J. Miner., Metall. Mater., 2016, 23(6), 723-729.

[16] Gao, X., Yue, H., Guo, E., Zhang, H., Lin, X., Yao, L., and Wang, B., "Preparation and tensile properties of homogeneously dispersed graphene reinforced aluminum matrix composites." Mater. Des., 2016, 94, 54-60.

[17] Radajewski, M., Henschel, S., Grützner, S., Krüger, L., Schimpf, C., Chmelik, D., and Rafaja, D., "Microstructure and mechanical properties of bulk TiN–AlN composites processed by FAST/SPS." Ceram. Int., 2016, 42(8), 10220-10227.

[18] Hayun, S., Paris, V., Mitrani, R., Kalabukhov, S., Dariel, M.P., Zaretsky, E., and Frage, N., "Microstructure and mechanical properties of silicon carbide processed by Spark Plasma Sintering (SPS)." Ceram. Int., 2012, 38(8), 6335-6340.

[19] Muthuchamy, A., Annamalai, A.R., Acharyya, S.G., Nagaraju, N., and Agrawal, D.K., "Microstructural and electrochemical behaviour of aluminium alloy composites produced using different sintering techniques." Mater. Res., 2018, 21(3), 1-7.

[20] Chang, Y.-h., Huang, D., Jia, C.C., Cui, Z.W., Wang, C.C., and Liang, D.,

"Influence of plasma on the densification mechanism of SPS under multi-field effect." Int. J. Miner., Metall. Mater., 2014, 21(9), 906-912.

[21] Nie, J.-h., Jia, C.C., Shi, N., Zhang, Y.F., Li, Y., and Jia, X., "Aluminum matrix composites reinforced by molybdenum-coated carbon nanotubes." Int. J. Miner., Metall. Mater., 2011, 18(6), 695-702.

[22] Tosun, G., and Kurt, M., "The porosity, microstructure, and hardness of Al-Mg composites reinforced with micro particle SiC/Al2O3 produced using powder metallurgy." Compos. Part B: Eng., 2019, 174, 106965.

[23] Agarwal, B.D., Broutman, L.J., and Chandrashekhara, K., Analysis and performance of fiber composites. 4th ed., India, John Wiley & Sons, 2017.

[24] Momohjimoh, I., Saheb, N., Hussein, M.A., Laoui, T., and Al-Aqeeli, N., "Electrical conductivity of spark plasma sintered Al2O3-SiC and Al2O3-carbon nanotube nanocomposites." Ceram. Int., 2020, 46(10), 16008-16019.

[25] Grigoriev, S., Peretyagin, P., Smirnov, A., Solis, W., Díaz, L.A., Fernández, A., and Torrecillas, R., "Effect of graphene addition on the mechanical and electrical properties of Al2O3-SiCw ceramics." J. Eur. Ceram. Soc., 2017, 37(6), 2473-2479.

[26] Aqida, S., Ghazali, M., and Hashim, J., "Effect of porosity on mechanical properties of metal matrix composite: an overview." J. Teknol., 2004, 17-32.

[27] Cramer, M. and Sevostianov, I., "Effect of pore distribution on elastic stiffness and fracture toughness of porous materials." Int. J. Fract., 2009, 160(2), 189-196.

[28] Jiang, B., and Weng, G., "A theory of compressive yield strength of nano-grained ceramics." Int. J. Plast., 2004, 20(11), 2007-2026.

[29] Nayak, K.C., and Date, P.P., "Hot deformation flow behavior of powder metallurgy based Al-SiC and Al-Al2O3 composite in a single step and two-step uni-axial compression." Mater. Charact., 2019, 151, 563-581.

[30] Jayakumar, K., Mathew, J., Joseph, M.A., Kumar, R.S., Shukla, A.K., and Samuel, M.G., "Synthesis and characterization of A356-SiCp composite produced through vacuum hot pressing." Mater. Manuf. Processes, 2013, 28(9), 991-998.

[31] Hossain, S., Rahman, M.M., Chawla, D., Kumar, A., Seth, PP., Gupta, P., Kumar, D., Agrawal, R., Jamwal, A., "Fabrication, microstructural and mechanical behavior of Al-Al2O3-SiC hybrid metal matrix composites." Mater. Today: Proc., 2020. 21 1458-1461.

[32] Dwivedi, S.P., Srivastava, A.K., Maurya, N.K., Sahu, R., Tyagi, A., and Maurya, R., "Microstructure and mechanical behaviour of Al/SiC/Al2O3 hybrid metal matrix composite." Mater. Today: Proc., 2020, 25, 789-792.

[33] Laszczyńska, A., Winiarski, J., Szczygieł, B., and Szczygieł, I., "Electrodeposition and characterization of Ni-Mo-ZrO2 composite coatings." Appl. Surf. Sci., 2016, 369, 224-231.

[34] Zamani, M., Amadeh, A., and Baghal, S.L., "Effect of Co content on electrodeposition mechanism and mechanical properties of electrodeposited Ni-Co alloy." Trans. Nonferrous Met. Soc. China, 2016, 26(2), 484-491.

[35] Feng, Q., Li, T., Teng, H., Zhang, X., Zhang, Y., Liu, C., and Jin, J., "Investigation on the corrosion and oxidation resistance of Ni–Al2O3 nano-composite coatings prepared by sediment co-deposition." Surf. Coat. Technol., 2008, 202(17), 4137-4144.

[36] Alizadeh, M., "Strengthening mechanisms in particulate Al/B4C composites produced by repeated roll bonding process." J. Alloys Compd., 2011, 509(5), 2243-2247.

[37] Beygi, R., Mehrizi, M.Z., and Eisaabadi B, G., "Friction stir processing of Al with mechanically alloyed Al-TiO2-Graphite powder: microstructure and mechanical properties." J. Mater. Eng. Perform., 2017, 26(3), 1455-1462.

[38]   Abe, F., Kern, T.-U., and Viswanathan, R., Creep-resistant steels. New York, Elsevier, 2008.

[39]   Liao, J.-z., Tan, M.-J., and Sridhar, I., "Spark plasma sintered multi-wall carbon nanotube reinforced aluminum matrix composites." Mater. Des., 2010, 31, 96-100.

[40]   Deng, C.F., Wang D.Z., Zhang X.X., and Li, A.B., "Processing and properties of carbon nanotubes reinforced aluminum composites." Mater. Sci. Eng. A, 2007, 444(1-2), 138-145.